Chapter 8
Delaminated Film Buckling Microchannels

Alex A. Volinsky and Patrick Waters

Abstract This chapter describes the method of manufacturing microfluidic microchannels formed by delaminated buckled thin films. Thin films under compression tend to delaminate and buckle. Microchannel geometry can be controlled by tailoring film residual stress and placing patterned adhesion-weakening layers utilizing photolithographic techniques. Results based on the photoresist as the adhesion weakening layer and compressed tungsten thin films are described along with the corresponding thin film mechanics.

8.1 Introduction

Buckling delamination blisters are commonly observed in compressed thin films. These mechanically active features arise from a local loss of adhesion between the film and the substrate, due to the relief of residual stress, and exhibit directional growth. Thin films in compression can also develop circular, asterisk, straight, and phone-cord blisters. "Telephone cords" are wormlike buckled features observed in thin films, and are called so because they look like a twisted phone cord when they are viewed under an optical microscope (Fig. 8.1). The geometry and path of these blisters can be controlled by placing adhesion-weakening layers, thereby outlining the desired in-plane blister configuration and forming a channel network on a chip.

Microfluidics, as a field, has been growing with the new advances in nanotechnology [1]. This field is estimated to grow at an exponential rate, and is expected to continue to do so in the decades to come. This relatively new technology has different possible applications, from sensors to drug delivery. It relies on the ability to transfer fluids at small-scale chip sizes. Recently these were successfully used to

A.A. Volinsky (✉) • P. Waters
Department of Mechanical Engineering, University of South Florida,
4202 E Fowler Ave ENB118, Tampa, FL 33620, USA
e-mail: volinsky@usf.edu

X. Chen (ed.), *Mechanical Self-Assembly: Science and Applications*,
DOI 10.1007/978-1-4614-4562-3_8, © Springer Science+Business Media New York 2013

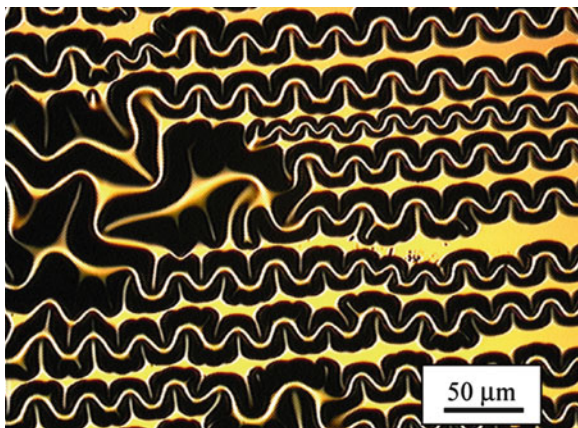

Fig. 8.1 Telephone cord buckling delamination of a compressed W film

deliver pharmacological agents directly to wound sites [2]. The channels used are commonly etched in silicon or other materials by means of standard methods of lithography. While it is not problematic to form an open trench, forming a channel is more complicated. There are multiple steps involved in the conventional technology [3], so the whole process is cumbersome, expensive, and labor intensive. In addition, Si is not biocompatible. Although one could envision a Si-based lab-on-a-chip device, the Si substrate has to be well isolated from the biological species and environment.

An alternative technology employs thin film delamination blisters which can form open micro- and nano-channel networks of specific geometry. Telephone cord delamination morphology is commonly observed as a result of the relief of residual compressive stresses within the thin film via interfacial debonding. Here, the biaxial film stress is partially relieved by film buckling in the direction perpendicular to the telephone cord propagation and by "secondary" blister buckling in the direction parallel to the telephone cord propagation. The combination of these types of buckling results in the observed sinusoidal fracture patterns [4, 5]. Normally, telephone cord blisters "run out of steam" and stop once the interfacial toughness exceeds the strain energy release rate. It is possible to make blisters propagate further by either putting mechanical energy into the system [5] or introducing liquids to the crack tip [6]. Inspired by recent results of moisture-induced thin film fracture [7], the thin film buckling delamination phenomenon was utilized as a way of manufacturing channel networks for the purposes of fluid transport in lab-on-a-chip devices and other microfluidic applications. In addition to forming channels, the thin film buckling delamination can act as a pump, thereby transporting the fluid during delamination. This allows for the enlargement of the channel cross section by using etching solutions during manufacturing.

Thin film and coating buckling delamination are truly multi-scale phenomena, with features possibly ranging from tens of nanometers to centimeters in width. In addition, compatibility with conventional microelectronic processing is very promising from the standpoint of full-scale on-chip integration. Crucial elements

of a lab-on-a-chip device are channels capable of transporting the fluids within the chip dimensions and an interface which is manipulatable from the outside world. Channels allow various fluids to be mixed, stored, and passed through. Typical fluids include blood, protein solutions in various buffers, cell suspensions, etc. Several measurements can be performed by microfluidic devices, including fluid viscosity and pH [8, 9].

The competitive advantage of the channel miniaturization is due to the fact that the Reynolds number is low, allowing for laminar flow to prevail and convective mixing of the fluids not to occur. Miniaturization of the channels, and their integration onto a single chip, would allow for the handling of minute amounts of sample material, thus increasing the sensitivity. The analyte concentration A_i is inversely proportional to its volume, V, and is given in terms of the device efficiency, η_s, as in [1]

$$A_i = \frac{1}{\eta_s N_{\mathrm{A}} V}, \tag{8.1}$$

where N_{A} is the Avogadro's number. Reduction of the sample size provides higher device sensitivity, as well as the capability of handling smaller samples. One can easily and effectively perform immuno- and DNA probe assays by using minute amounts of sample material.

In addition, the channel profile geometry has a substantial influence on the fluid flow. It is important to know the distribution of the analytes in the channel for developing functional and reproducible assays. One would want to increase the molecule residence time for quantitative time-dependent analyses. The prediction of the molecule residence time is a complicated task, as it depends on the molecule location in the channel profile. A low-aspect-ratio channel velocity profile allows lateral diffusion to occur in the vertical dimension without an accompanying change in the residence time of the diffusing molecules. Therefore, one would desire microchannels with low aspect ratios for accurate quantitative studies. Thin film buckling channels have a low aspect ratio, i.e., height-to-width ratio.

8.2 Thin Film Buckling Delamination

Many industries, including microelectronics and microfluidics, depend on well-adhered thin films. Thin films are normally stressed, with biaxial residual stress residing in unpassivated films [10]. Stress in a thin film typically causes substrate bending. This effect is employed in measuring the macroscopic residual stress found within thin films by using Stoney's equation [11]. There are many different stress relief mechanisms observed in thin films. The residual stress can be partially relieved by plastic deformation and surface reconstruction. It may also be more completely relieved by mechanical film failure, especially if the stress levels are high and/or externally applied stresses are present.

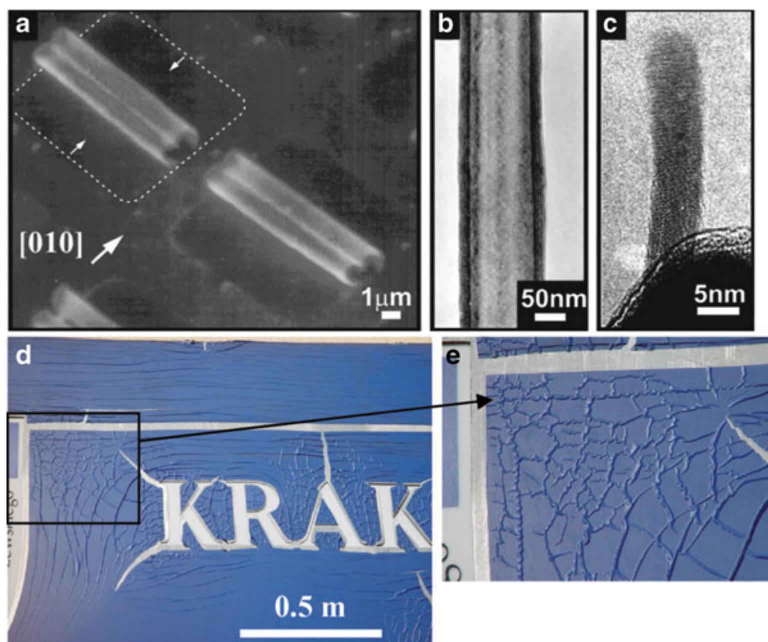

Fig. 8.2 (**a–c**) SEM and HRTEM images of InGaAs/GaAs nanotubes rolled up from bi-layered films: (**a**) Two scrolled single walls; (**b**) multi-wall nanotube (6 turn, film thickness: 4ML GaAs +4ML InGaAs); (**c**) single-wall nanotube formed from 2ML GaAs + 1ML InAs. Reprinted with permission from [23, 24]; (**d**) and (**e**) Polymer film buckling delamination on a street sign due to seasonal temperature variations. Waters and Volinsky [31], reprinted with permission

Telephone cord delamination has been observed in various thin film systems, including tungsten, carbon, diamond-like carbon (DLC), TaN, and other films which have been applied upon various substrates [12–18]. Some theoretical considerations of the formation of the telephone cord buckling geometry can be found in [19–22]. Most of the time delamination blisters run parallel to each other in blanket, non-patterned films (Fig. 8.1). The multi-scale nature of these phenomena can be seen in Fig. 8.2a–e. Figure 8.2a–c shows ultrathin films (several monolayers—ML) rolling into nanotubes [23, 24], while Fig. 8.2d–e shows polymer film buckling delamination on a street sign, several meters long, induced by seasonal temperature fluctuations, thereby causing the film buckling and adhesion loss. Telephone cord delamination morphology is commonly observed as a result of the thin film residual compressive stress relief by interfacial debonding (Fig. 8.3).

If the residual stress is less than four times the buckling stress, straight blisters become possible under biaxial residual compressive stress. However, this level of residual stress may not be high enough to initiate delamination. That is why residual stress-induced straight blisters are rarely observed in thin films. This situation changes, however, when the stress is applied externally, or when the adhesion is somehow weakened. A simple experiment with a compact disc (CD) in 3-point

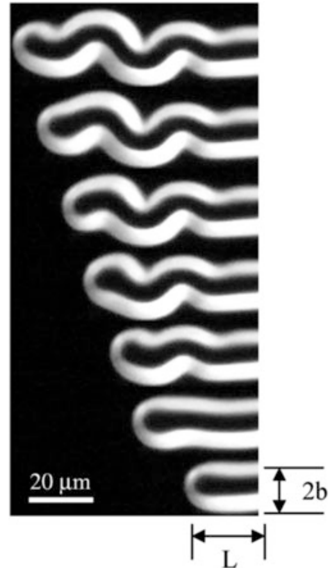

Fig. 8.3 Transition from straight-sided blister to sinusoidal shape

bending has been described in [4] to support this. Detailed dynamics of real-time telephone cord blister propagation can be observed online [25]. As was previously stated, telephone cord blisters "run out of steam" and stop once the interfacial toughness exceeds the strain energy release rate. It is possible to make blisters propagate further by either putting mechanical energy into the system [5] or introducing liquids at the crack tip [6, 7]. Liquids can also provide the mechanical energy (through surface tension and capillary forces) needed to continue the blister propagation and can also reduce the film interfacial toughness. These effects were attributed to environmentally assisted cracking, which caused the thin film delamination, and is similar to a commonly known example of the degradation and fading of vintage mirrors, as well as solar mirrors [26]. If one were to use a substrate etching solution as a fluid, then, in addition to causing thin film delamination, it would etch the substrate, thereby enlarging the channel cross section.

Tests have been conducted that demonstrate the method of fluid introduction as a means of propagating delamination blisters. These blisters continue to propagate until the fluid has been removed, or until the delamination reaches the end of the sample [6]. All of the samples contained a 1 µm thick W superlayer deposited on either thin magnetic layers or 40 nm thick Cu films on Si substrates, with a thermally grown SiO_2 layer. Figure 8.4 shows two snapshots, taken 3 min apart, illustrating water-induced blister propagation. The evidence of fluid transport is presented in Fig. 8.5. Here, the buckling delamination propagated from the right to the left, and the water, upon reaching the far left side of the sample, moved down the edge of the Si wafer. This demonstrates one of the potential mechanisms of fluid transport via blister propagation. In this case, water was transported, with the advance of the crack tip, at about 10 µm/min, although higher propagation rates,

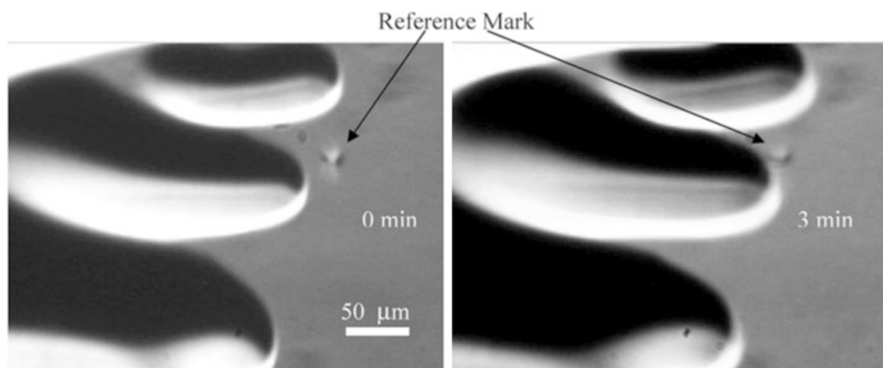

Fig. 8.4 Water-induced blister growth. Volinsky et al. [7], reprinted with permission

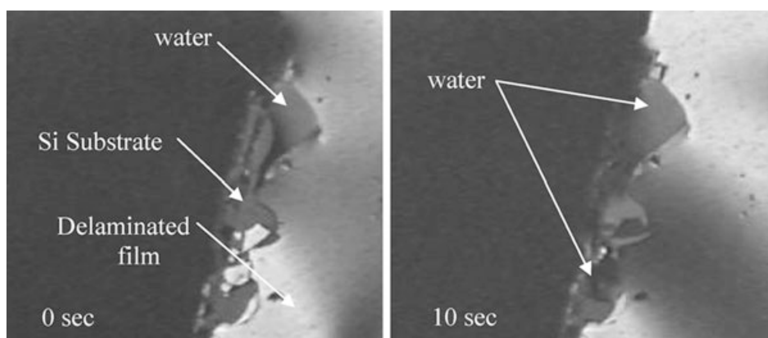

Fig. 8.5 Water transport in the delaminated blister. Volinsky et al. [7], reprinted with permission

up to several microns per second, were observed in other samples. It has been previously shown that interfacial cracks in thin films act as a vacuum cleaner, collecting contaminants from the atmosphere, thus reducing the energy of the newly formed fracture surfaces [13, 14]. In this case, the crack is acting like a pump, thus transporting the fluid along with the blister propagation. Water droplets can be seen on the Si substrate in Fig. 8.5.

In order to make a microfluidic or lab-on-a-chip device, the placement of delamination fluid transport channels needs to be exact and repeatable. Standard lithographic techniques have demonstrated the ability to control the blister placement and the buckling geometry [27]. Both telephone cord as well as straight blister geometries are available and depend on the film stress level and the width of the adhesion-weakening (release) layer [27]. With the use of moisture, the requirements on the release layer adhesion properties are less stringent, as the stress combined with the moisture is sufficient to cause delamination. The properties of the internal walls of the channel can be altered by varying the underlying materials. For example, it has been shown that fracture in low-K dielectric films is

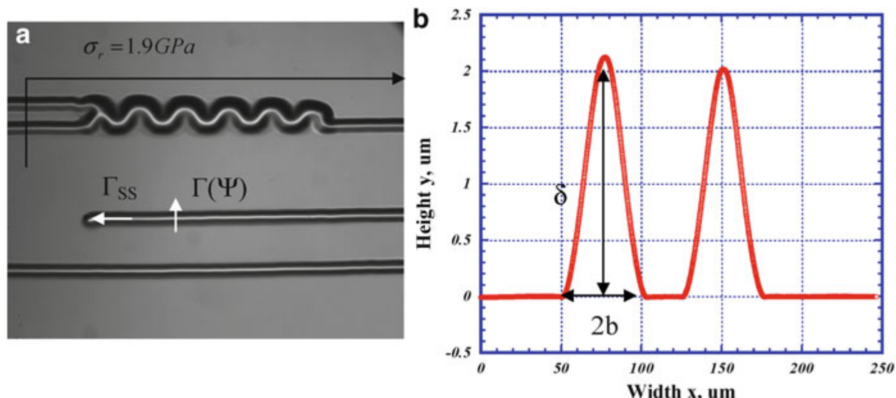

Fig. 8.6 (**a**) Optical micrograph of two straight buckled channels coalescing into one through a telephone cord delamination, and (**b**) corresponding height profiles. Volinsky et al. [7], reprinted with permission

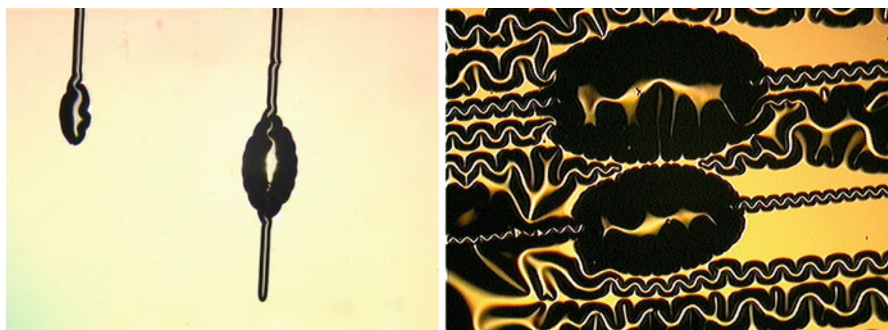

Fig. 8.7 Buckling delamination showing channels and fluid "storage reservoirs"

cohesive, i.e., the crack propagates in the film itself [28]. A similar effect is expected for a polymer release layer and it may even be possible to use regular photoresistant "lining" inside the channel. One could also use a biocompatible material as an adhesion-weakening layer, which would include polymer and ceramic films, as well as DLC.

Figure 8.6a shows two 50 μm wide straight channels, which coalesce by forming a telephone cord delamination blister, resulting in a single 50 μm wide channel. The profilometer scan in Fig. 8.6b reflects the blister buckling geometry. A highly desirable microchannel aspect ratio of 1:25 is achieved here. This demonstrates the possibility of constructing a fluid-mixing device by employing thin film buckling channels. In this particular case, the double-to-single channel transition occurred naturally, although the same result can be achieved with patterned release layers, which form channel network structures. Another important example of a storage element is shown in Fig. 8.7, where a channel extends to a larger reservoir.

One can envision using this storage element as a pump, when combined with an electrostatic device capable of mechanically pressurizing it from the top.

8.3 Buckling Blister Mechanics

The buckling channel geometry can be predicted based on the multilayer material properties, residual stress, and adhesion [22]. The steady-state interfacial toughness of the film, in the direction of the blister propagation (shown in Fig. 8.6a), is

$$\Gamma_{SS} = \frac{(1-v^2)h\sigma_r^2}{2E}\left(1-\frac{\sigma_B}{\sigma_r}\right)^2, \tag{8.2}$$

where σ_r and σ_B are the residual (compressive) stress and the buckling stress, respectively, h is the film thickness, E is the elastic modulus, and v is the Poisson's ratio. The buckling stress is given in terms of the film thickness and the blister width, b, as

$$\sigma_B = \frac{\pi^2}{12}\frac{E}{(1-v^2)}\left(\frac{h}{b}\right)^2. \tag{8.3}$$

Now one can express the residual stress in terms of the buckling stress and the blister heights, δ, as

$$\sigma_r = \frac{3}{4}\sigma_B\left(\frac{\delta^2}{h^2}+1\right). \tag{8.4}$$

To complete the formulation, the mode-dependent interfacial film toughness, in the buckling direction, perpendicular to the blister propagation, can be expressed as

$$\Gamma(\Psi) = \frac{(1-v^2)h}{2E}(\sigma_r-\sigma_B)(\sigma_r+3\sigma_B). \tag{8.5}$$

This simple analysis basically shows that the level of the residual stress and the extent of the thin film adhesion will control the microchannel geometry. The upper layer residual stress, determined primarily by the deposition parameters, will control the microchannel height.

Typically, residual stress in thin films results in negative consequences that include wafer bowing, film cracking, and delamination. However, depositing a film with a compressive residual stress has been demonstrated to be a benefit, specifically when using superlayer indentation to determine the thin film interfacial toughness [12]. A similar concept can be employed to create microchannels. When the strain energy release rate, G, exceeds the interfacial toughness, Γ_i, of a film/

substrate, delamination will occur. A simplified form of the strain energy release rate in a stressed film is [22]

$$G = Z\frac{\sigma_{\mathrm{f}}^2 h}{E_{\mathrm{f}}}, \tag{8.6}$$

where σ_{f} is the stress in the film, h is the film thickness, E_{f} is the modulus of elasticity, and Z is a dimensionless parameter that depends on the geometry.

In thin film systems with biaxial compressive stresses, various shapes of the delaminated regions will arise. These shapes include long straight-sided, circular, and telephone cord delamination, which is the most commonly observed morphology. The delamination shape and size will depend on factors such as the film stress, thickness, and interfacial toughness. Most importantly, the propagation depends on the interfacial toughness, which increases as the mode mixity, acting on the interface ahead of the delamination crack, shifts from mode I towards mode II. Interfacial failure starts with the film delaminating from the substrate and is followed by the spreading of the delamination as the buckling loads the edge of the interfacial crack, resulting in a failure phenomenon that couples both buckling and interfacial crack propagation.

To create useful microchannels via film delaminations, the direction and morphology of the delaminations need to be controlled. The easiest way to control delamination is by controlling the interfacial toughness. This can be done by creating adhesion-reducing layers that have a lower interfacial toughness than the surrounding areas. A compressively stressed film can be used in conjunction with a patterned adhesion-reducing layer as a method for creating microchannels. Using delaminations will hopefully solve the existing challenges and provide an alternative method in creating microchannels.

8.4 Buckling Microchannel Pattern Manufacturing

To create the adhesion-reducing layers, standard photolithography techniques were employed [29]. The simplest approach used the patterned photoresist as the adhesion reducer. The basic steps in lithography include the following:

(1) The application of a photosensitive material (photoresist)
(2) Soft bake of the photoresist
(3) Exposure of the photoresist
(4) Development of the exposed pattern
(5) Hard bake of the remaining pattern

Figure 8.8 is a depiction of the basic lithography steps used here, along with the additional step of depositing a compressively stressed film for creating delamination-induced microchannels.

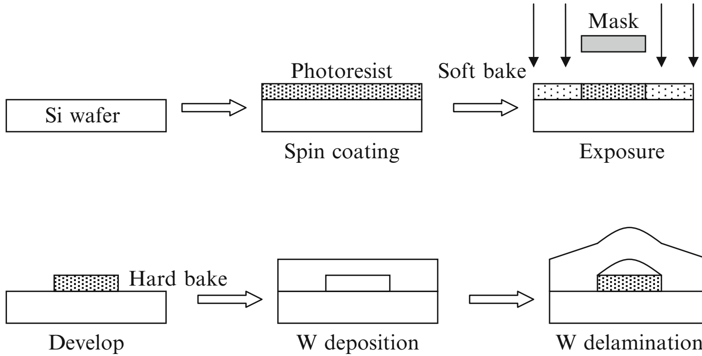

Fig. 8.8 Process of creating microchannels

There are two types of photoresist to choose from: positive and negative photoresist. Positive photoresist is exposed to UV light wherever it is to be removed. Regarding the positive photoresist, exposure to the UV light changes its chemical structure so that it becomes more soluble in a developer, which is opposite to that of the negative photoresist. The exposed photoresist is then washed away by a developer solution, leaving areas of the underlying material bare. Therefore, the mask contains an exact copy of the pattern, which is to remain on the wafer. In general, positive photoresists provide clearer edge definition than negative photoresists. The better edge definition found in positive photoresists makes them a better option for high-resolution patterns.

Negative photoresists behave in the opposite manner. Exposure to the UV light causes the negative photoresist to become polymerized, and consequently more difficult to dissolve. Therefore, the negative photoresist remains on the surface wherever it is exposed, and the developer solution removes only the unexposed portions. Thus, masks used for negative photoresists contain the inverse of the pattern to be transferred. Shipley 1813 was used here, which is a positive photoresist that is optimized for G-line exposure (436 nm wavelength).

Normally, to start the photoresist application process, the wafer surface is prepared in a specific way in order to remove the surface moisture and other contaminants. In order to remove the moisture, the wafers are baked and then primed with an adhesion promoter. Hexamethyldisilazane (HMDS) is normally used as the adhesion promoter and is applied at a reduced pressure to form a monomolecular layer on the wafer surface, thereby making the wafer hydrophobic, which prevents moisture condensation. These wafer preparation steps were ignored here because the goal of the photoresist layer was to be an adhesion reducer and only a proof of concept was intended.

Spin coating was used to apply the photoresist with thicknesses ranging from a few hundred nanometers to a few microns. If thicker coatings are required, electrochemical coatings, spray coatings, and casting processes can be used [29]. A Laurell Technologies WS-400A-8NPP/Lite Spin Processor was utilized here and can handle wafers up to 8″ in diameter. It uses a vacuum chuck to hold the

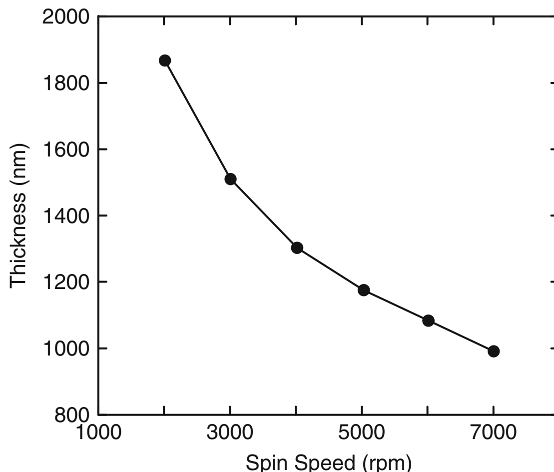

Fig. 8.9 Photoresist thickness as a function of spin speed for Shipley 1813

wafers in place and has a spin speed which can range from 0 to 6,000 rpm. Acceleration profiles, speed changes, and spin times can all be programmed by the user. By adjusting the spin speed, the photoresist thickness can be controlled. The manufacturer-supplied thickness versus spin speed data for the Shipley 1813 is shown in Fig. 8.9. They suggest that the Shipley 1813 has the best coating uniformity between spin speeds of 3,500 and 5,500 rpm.

The spin speed and time used here were 4,000 rpm for 40 s, with a ramp speed of 1,000 rpm/s. Based on the manufacturer's supplied data for the photoresist thickness versus spin speed, it was expected to have a photoresist thickness of approximately 1.3 μm after application. However, the resist thickness was measured to be approximately 1.5 μm with relatively good thickness uniformity across the wafer diameter. Spin-on deposition of the photoresist was a tricky process because the photoresist was applied manually. First, the wafer surface had to be thoroughly cleaned of any debris to avoid streaking of the photoresist during spinning. After the surface cleaning, the wafer had to be centered on the vacuum chuck to avoid uneven distribution of the photoresist. A drop of photoresist was then placed in the center of the wafer and a few additional drops were added during the first 5 s, in which the spin speed of the wafer was ramped to the maximum rpm. Upon completion of the spin-on deposition, the wafer was placed on a hot plate for 90 s at 90 °C.

After the photoresist soft bake, a range of exposure times were attempted in order to find the optimum photoresist thickness. The light source used for the photoresist exposure was a mercury vapor lamp, which provides a wavelength spectrum from 310 to 440 nm. A Karl Suss MA 56 Mask Aligner was used in hard contact mode for the mask and wafer alignment. The mask had a repeating pattern, which consisted of two straight lines running parallel, where the line width was measured to be 250 μm with 30 μm separation. The results of the photoresist profiles, after testing a range of exposure times, can be seen in Figs. 8.10 and 8.11. The photoresist width and thickness varied by up to 10% across the 4″ wafer diameter.

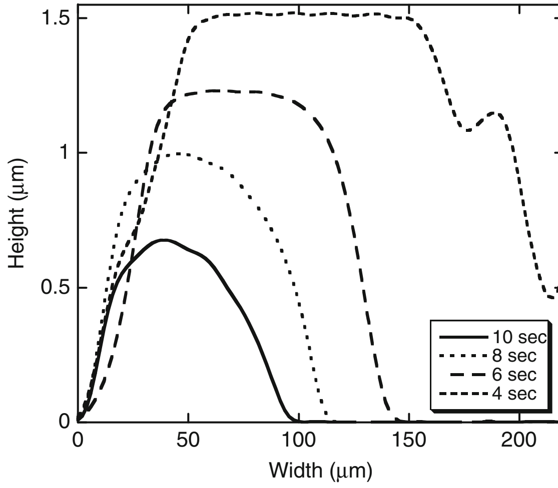

Fig. 8.10 Photoresist profiles after different exposure times

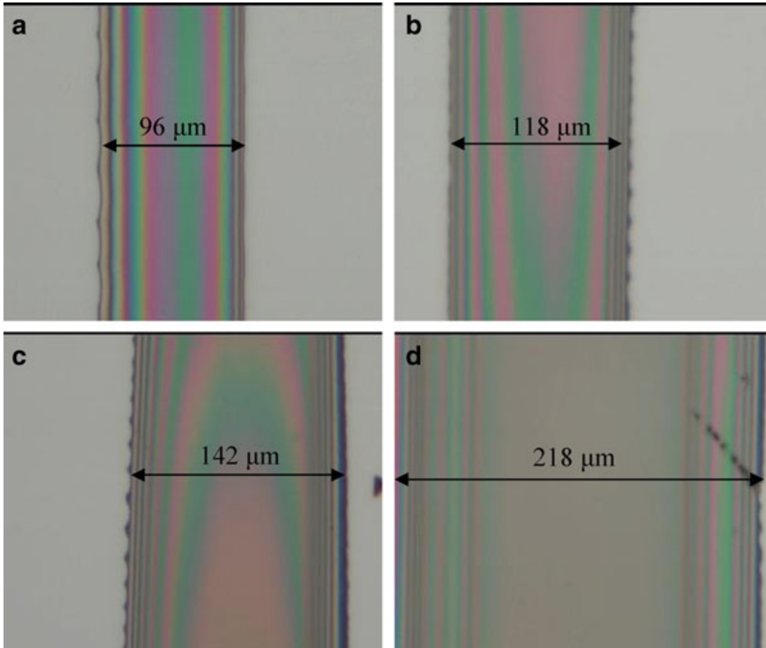

Fig. 8.11 Effect of exposure time on the final photoresist thickness: (**a**) 10 s, (**b**) 8 s, (**c**) 6 s, and (**d**) 4 s

At the shortest exposure time of 4 s, the remaining developed photoresist measured 1.5 μm in height and 218 μm in width. However, on most of the wafer there also remained a thinner layer of photoresist between the parallel lines. It was concluded that an exposure time of 4 s at 275 W was inadequate. From there the exposure time was increased by 2-s increments, with the final resist height and width being inversely proportional to the exposure time. Along with decreasing line height and width, the resist profile ended up being more rounded as the exposure time was increased.

After exposure, the wafers were placed in a developer bath for 30 s and were then rinsed with deionized water. Nitrogen was used to remove the majority of the excess moisture on the wafer, which was then hard baked on a hot plate at 110 °C for 100 s.

Overall, the lithography techniques used here were adequate in accomplishing the objective of creating simple patterns on a wafer. However, a more thorough approach can be taken in the future for optimizing spin speed and time, bake time and temperature, and exposure and development time. It must be understood that the line widths created here are relatively large when compared with other lithography techniques. Therefore, the quick optimization steps used here were adequate. If smaller line widths and heights were required, a more meticulous approach would be needed. The final step in the process was to deposit a tungsten film that is forced to have compressive residual stress.

8.5 Buckling Delamination Morphology

The various shapes of buckled regions evolve in film/substrate systems that are in a state of biaxial compression. Details of their shape and size will depend on factors such as the film stress, thickness, and interfacial toughness. The buckling geometry can be used to assess the interfacial toughness. Figure 8.12 is a picture of three straight-sided delaminations of a tungsten and DLC film stack on a silicon wafer.

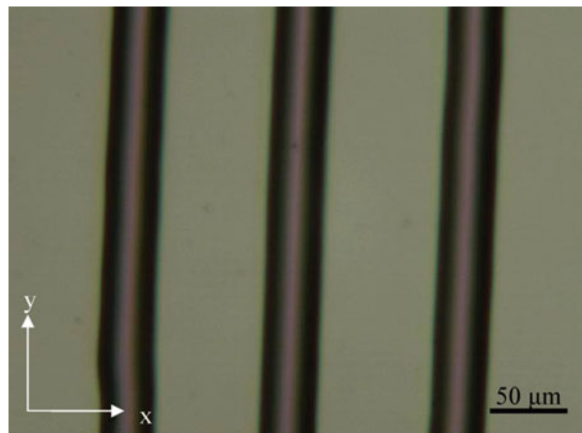

Fig. 8.12 Straight-sided delaminations of a W/DLC film on Si

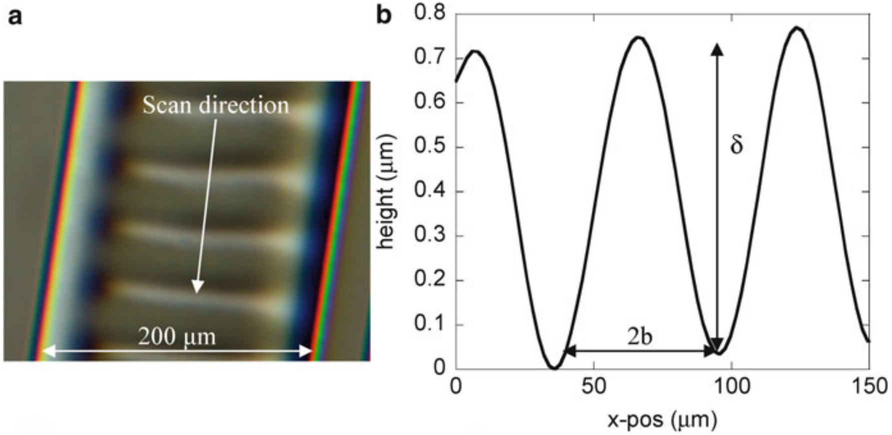

Fig. 8.13 Tungsten delamination: (**a**) Optical image of delamination morphology and (**b**) Profile of delaminations

Assuming that fracture happens at the interface, (8.2) through (8.5) can be applied to solve for the interfacial toughness between the photoresist and the tungsten film, when straight-sided delaminations are present. One of the initial deposition tests was on a silicon wafer patterned with the larger 200 μm wide photoresist lines. The tungsten film was deposited for 50 min with an argon pressure of 5 mTorr. This resulted in straight-sided delaminations forming across the width of the photoresist line, as shown in Fig. 8.13a. The profile of the straight-sided delamination widths is shown in Fig. 8.13b. Using the delamination height, δ, the delamination half width, b, and (8.2)–(8.5), the critical buckling stress was calculated to be 194 MPa. The residual stress of the film was found to be 313 MPa, the steady-state interfacial toughness was found to be 0.0114 J/m^2, and the mode-dependent interfacial toughness was found to be 0.0859 J/m^2.

The steps taken for calculating the interfacial toughness assumed that fracture took place at the tungsten/photoresist interface. There is a possibility that the crack propagates in the photoresist, at the interface between the photoresist and the silicon substrate, or a combination of above mentioned. No matter where the crack is propagating, however, the important thing is that the interfacial toughness between the tungsten film and the silicon substrate, which has been reported in literature to be 1.73 J/m^2 [30], is stronger than that measured in the photoresist areas.

Moon et al. have found that the delamination morphology can be predicted when the film stress is compared to the buckling stress [27]. For $\sigma_r/\sigma_B < 6.5$ straight-sided delaminations are predicted and for $\sigma_r/\sigma_B > 6.5$ telephone cord delaminations are predicted. For the delaminations shown in Fig. 8.13, $\sigma_r/\sigma_B = 1.6$, which agrees with the Moon et al. findings. Their predictions of delamination morphology were based on similar experimental methods that utilized lithography techniques in applying patterned areas of low interface adhesion surrounded by areas of high adhesion. By controlling the width of the low-adhesion strips, the buckle morphology was controlled.

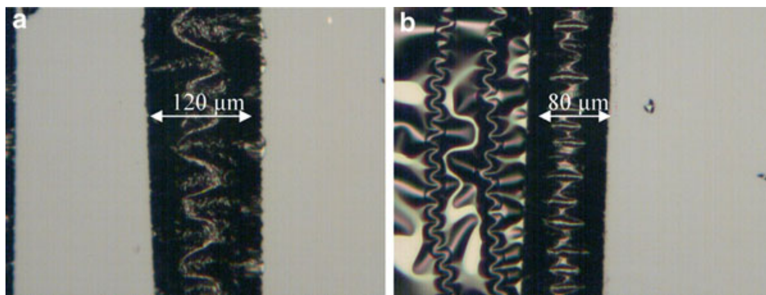

Fig. 8.14 Delamination morphology with different photoresist widths: (**a**) Telephone cord delamination and (**b**) straight-sided delamination

Ideally the delaminations would propagate parallel to the photoresist lines as opposed to perpendicular to them, as seen in Fig. 8.13. The main reason in preventing this from happening is that the photoresist line is too wide. The photoresist is so wide that it exceeds the critical buckling width, thereby allowing enough room for the straight-sided delaminations to run perpendicular to the lines. Figure 8.14 shows two different delamination morphologies that are possible when the photoresist line is decreased in width. Telephone cord delamination morphology can be observed in Fig. 8.14a when the photoresist width was approximately 120 μm. When the photoresist width was reduced to approximately 80 μm, as shown in Fig. 8.14b, a straight-sided delamination was created. Unfortunately, as shown in Fig. 8.14b, tungsten delamination also occurred in between the photoresist lines.

The delamination morphology that was observed in Fig. 8.14 would be necessary if the delaminations were to find future use in transporting fluids. Continued work is necessary to further experiment with photoresist width and its effect on delamination morphology. Attention to deposition parameters, in regard to controlling the residual stress, was found to be more important when using the adhesion-reducing layers. Not only was delamination occurring in the patterned areas, but it was also common to see the delamination propagate across other areas of the wafer. The adhesion-reducing areas acted as crack initiation sites that helped spawn delamination upon film deposition. There appears to be a fine line between creating delaminations on the patterned areas and creating them on the rest of the wafer. Controlling the exact amount of compressive residual stress is critical for this method to succeed in the consistent creation of microchannels.

8.6 Conclusions and Outlook

By using photolithography to create adhesion-reducing layers, buckling delaminations have been controlled and show potential use as microchannels. Delamination morphology depends on two conditions: (1) the buckling stress

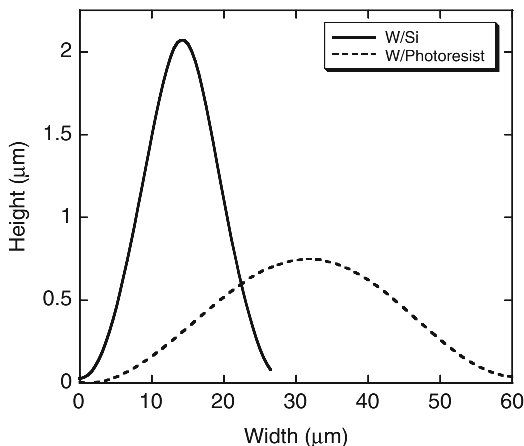

Fig. 8.15 Different delamination channel profiles

which is controlled by the adhesion-reducing layer's width and (2) the amount of compressive residual stress in the thin film. Here, telephone cord delaminations were observed at larger photoresist widths and straight-sided delaminations were observed for smaller photoresist widths. Line widths between 80 and 220 μm were created.

By using standard lithography techniques, areas of low adhesion were created to control delamination morphology. This could be used as a new method for creating microchannels for transporting, mixing, and storing fluids in microfluidic devices. Current methods for creating microchannels involve etching and wafer bonding. The potential advantages of this new method are found in its ease of manufacturing and its cost-effectiveness. Proof of concept was provided here by using a photoresist as the adhesion-reducing layer. By controlling the photoresist line width, the delamination morphology was consequently controlled.

Microfluidics has been a rapidly growing field, along with the rest of the microelectronics boom. In the late 1980s the early stages of microfluidics were dominated by the development of microflow sensors, micropumps, and microvalves [1]. Like many different areas of engineering, having everyone agree on a set definition is sometimes difficult. Microfluidics does not differ in this regard. One point that the majority can agree upon is that a microscopic quantity of fluid is the key issue in microfluidics. One main advantage of microfluidics is utilizing scaling laws for achieving better sensor performance. As the fluid volume is decreased, there will also be a need to decrease the size of the channels the fluid is transported in. Some possible delamination sizes created here are shown in Fig. 8.15. The delamination channel width was varied from 25 to 60 μm and the height was varied from 0.75 to 2 μm.

An interesting effect has been observed with the introduction of water at the film/substrate interface of highly compressed films. Water appears to reduce interfacial toughness, thereby allowing for the initiation of spontaneous delamination propagation. Figure 8.16 shows the propagation of a telephone cord delamination, over a

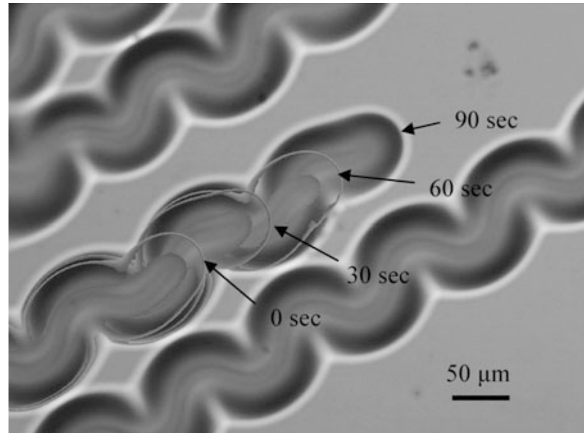

Fig. 8.16 Delamination propagation induced by the introduction of water. Waters and Volinsky [31], reprinted with permission

90-s time interval, when water was introduced at the lower left-hand corner [31]. In this case (Fig. 8.16), the delamination microchannels could be used as a one-time use, disposable microfluidic device.

Using film delaminations to create microchannels shows promise in the field of microfluidics. The key to creating the microchannels is in utilizing areas of reduced adhesion to control the delamination morphology. Possible areas for future work could be in finding better choices for adhesion-reducing layers and developing more complex delamination patterns. Creating the microchannels is only a small component of the overall picture if they are to be used in microfluidic devices. Integration of the microchannels onto a “lab-on-a-chip”-type device [32] is the overall goal, but many questions still need to be answered on how the fluid will be placed into the microchannels and how the fluid will be transported once inside the microchannels.

References

1. Nguyen NT, Werely ST (2002) Fundamentals and applications of microfluidics, Artech House, Norwood, MA,1–19:285–286
2. Spence A, Retterer S, Isaacson M (2002) Microfabricated model silicon probes with microfluidic, channels for drug delivery. NNUN Abstracts 2002/Biology & Chemistry, p 13
3. Li Y, Gulari MN, Wise KD (2003) High-yield buried microchannel formation for drug delivery at the cellular level, In: Northrup MA, Jensen KF, Harrison DJ (eds) Proceedings of mTAS 2003 seventh international conference on micro total analysis systems, vol 2, October 5–9, Squaw Valley, CA, pp 931–934
4. Volinsky AA (2003) Experiments with in-situ thin film phone cord delamination propagation. Mat Res Soc Symp Proc 749:W10.7
5. Volinsky AA, Meyer DC, Leisegang T, Paufler P (2003) Fracture patterns in thin films and multilayers. Mat Res Soc Symp Proc 795:U3.8
6. Volinsky AA, Waters P, Kiely JD, Johns EC (2005) Sub-critical telephone cord delamination propagation and adhesion measurements. Mat Res Soc Symp Proc 854E:U9.5

7. Volinsky AA, Waters P, Wright G (2004) Micro-fluidics applications of telephone cord delamination blisters. Mat Res Soc Symp Proc 855E:W3.16
8. Galambos P (1998) Two-phase dispersion in micro-channels. Ph.D. Thesis, Mechanical Engineering, University of Washington, Seattle
9. Macounova K, Cabrera CR, Holl MR, Yager P (2000) Generation of natural pH gradients in microfluidic channels for use in isoelectric focusing. Anal Chem 72:3745–3751
10. Ohring M (1992) The materials science of thin films. Academic, London
11. Stoney GG (1909) The tension of metallic films deposited by electrolysis. Proc Roy Soc Lond A82:72
12. Volinsky AA, Moody NR, Gerberich WW (2002) Interfacial toughness measurements for thin films on substrates. Acta Mater 50(3):441
13. Volinsky AA, Moody NR, Kottke ML, Gerberich WW (2002) Fiducial mark and nanocrack zone formation during thin film delamination. Philos Mag A 82:3383–3391
14. Volinsky AA, Moody NR, Gerberich WW (2003) Fiducial mark and CTOA estimates of thin film adhesion. Int J Fract 119(4):431–439
15. Matuda N, Baba S, Kinbara A (1981) Internal stress, Young's modulus and adhesion energy of carbon films on glass substrates. Thin Solid Films 81:301
16. Gille G, Rau B (1984) Buckling instability and adhesion of carbon layers. Thin Solid Films 120:109
17. Seth J, Raghunath R, Babu SV (1992) Influence of the deposition gas mixture on the structure and failure modes of diamondlike carbon films. J Vac Sci Technol A 10(2):284–289
18. Moon M-W, Jensen HM, Hutchinson JW, Oh KH, Evans AG (2002) The characterization of telephone cord buckling of compressed thin films on substrates. J Mech Phys Solids 50 (11):2355
19. Thouless MD (1990) Crack spacing in brittle films on elastic substrates. J Am Ceram Soc 73:2144
20. Bai T, Pollard DD, Gao H (2000) Explanation for fracture spacing in layered materials. Nature 403:753
21. Huang R, Prevost JH, Huang ZY, Suo Z (2003) Channel-cracking of thin films with the extended finite element method. Eng Fract Mech 70(2513)
22. Hutchinson JW, Suo Z (1992) Mixed-mode cracking in layered materials. Adv Appl Mech 29:63–191
23. Prinz VY (2000) Free-standing and overgrown InGaAs/GaAs nanotubes, nanohelices and their arrays. Physica E 6(1–4):828–831
24. Prinz VY (2004) Precise semiconductor nanotubes and nanoshells fabricated on (110) and (111) Si and GaAs. Physica E 23:260–268
25. World Wide Web: http://www.eng.usf.edu/~volinsky
26. Burolla VP (1980) Deterioration of the silver/glass interface in second surface solar mirrors. Sol Energy Mater 3/1–2:117–126
27. Moon MW, Lee KR, Oh KH, Hutchinson JW (2004) Buckle delamination on patterned substrates. Acta Mater 52/10:3151–3159
28. Volinsky AA, Vella JB, Gerberich WW (2002) Fracture toughness, adhesion and mechanical properties of low-K dielectric thin films measured by nanoindentation. Thin Solid Films 429 (1–2):201–210
29. Franssila S (2004) Introduction to micro fabrication. Wiley, West Sussex, England
30. Kriese MD, Gerberich WW, Moddy NR (1999) Quantitative adhesion measures of multilayer films: Part II. Indentation of W/Cu, W/W, Cr/W. J Mater Res 14(7):3019
31. Waters P, Volinsky AA (2006) Stress and moisture effects on thin film buckling delamination. Exp Mech 47(1):163–170
32. Weigl BH, Hedine K (2002) Lab-on-a-chip-based separation and detection technology for life science applications. Am Biotechnol Lab 20(1):28–30